Hydrol. Earth Syst. Sci. Discuss., https://doi.org/10.5194/hess-2017-723
Manuscript under review for journal Hydrol. Earth Syst. Sci.
Discussion started: 19 December 2017

Hydrology and Earth System Sciences
Open Access
Discussions

Testing an optimality-based model of rooting zone water storage capacity in temperate forests

Matthias J.R. Speich[1,2,3], Heike Lischke[1], Massimiliano Zappa[2]

[1]Dynamic Macroecology, Swiss Federal Research Institute WSL, 8903 Birmensdorf, Switzerland
[2]Hydrological Forecasts, Swiss Federal Research Institute WSL, 8903 Birmensdorf, Switzerland
[3]Department of Environmental Systems Science, ETH Zurich, 8092 Zurich, Switzerland

Correspondence to: Matthias Speich (matthias.speich@wsl.ch)

Abstract. Rooting zone water storage capacity S_r is a crucial parameter in models of hydrology, ecosystem gas exchange and vegetation dynamics. Despite its importance, this parameter is still poorly constrained and subject to high uncertainty. We tested the analytical, optimality-based model of effective rooting depth proposed by Guswa (2010) with regard to its applicability for parameterizing S_r in temperate forests. The model assumes that plants dimension their rooting systems in order to maximize net carbon gain. Results from this model were compared against values obtained by calibrating a local water balance model against latent heat flux and soil moisture observations from 15 eddy covariance sites. To increase the applicability of the rooting depth model, we provide a numerical approximation of its underlying probabilistic soil moisture model.

The calibration and validation of the local water balance model showed that the concept of a single rooting zone storage capacity was appropriate at most temperate and cold sites, but not at Mediterranean sites and for very coarse soils. At a majority of sites, the estimates of S_r are generally in good agreement. However, mismatches were found in stands dominated by Norway spruce, especially at high elevations. These mismatches were attributed to the fact that the model does not consider rooting depth limitations due to oxygen stress and low soil temperature. Also, it is not clear whether the rooting behavior of pines on coarse soils is captured properly. Nevertheless, the overall good agreement suggests that this model may be useful for generating estimates of rooting zone storage capacity for both hydrological and ecological applications. Another potential use is the dynamic parameterization of the rooting zone in process-based models, which greatly increases the reliability of transient climate-impact assessment studies.

1 Introduction

Rooting zone storage capacity S_r, expressing the maximum amount of water that can be stored in the soil and accessed by plants, is a crucial variable for the water balance and vegetation dynamics of terrestrial ecosystems. From a hydrological point of view, S_r governs the partitioning of rainfall into transpiration and water yield (Milly, 1994), so that an increase in S_r leads to an increase in long-term transpiration (Federer et al., 2003) and a decrease in long-term runoff (Donohue et al.,

Hydrol. Earth Syst. Sci. Discuss., https://doi.org/10.5194/hess-2017-723
Manuscript under review for journal Hydrol. Earth Syst. Sci.
Discussion started: 19 December 2017

Hydrology and Earth System Sciences
Open Access
Discussions

2012). Also, as S_r constrains transpiration, it may limit biological productivity (Porporato et al., 2004). Furthermore, S_r is also an important variable controlling water, carbon and energy fluxes at the Earth's surface in climate models (Kleidon and Heimann, 1998; Wang and Dickinson, 2012).

Although its importance has long been recognized, S_r is still a poorly constrained parameter. As S_r is not a directly observable quantity, it is difficult to relate it to field measurements. An often-used useful simplification (Federer et al., 2003; Kleidon and Heimann, 1998) is the definition of S_r (expressed in mm water depth) as the product of the water-holding capacity κ [mm mm^{-1}] of the soil (i.e. the difference between soil water content at field capacity and at the wilting point) and the effective rooting depth Z_e [mm], defined as the lowest depth in the soil profile where water is still accessible to roots. While κ is generally assumed to remain constant, some approaches focus on estimating Z_e to parameterize S_r. Given that soil properties and rooting patterns vary at spatial scales much smaller than typical spatial discretization units in hydrological and ecosystem models (such as a catchment, grid cell or forest stand), κ and Z_e are usually taken as spatial averages. For this reason, point-scale observations of rooting depth cannot be assumed to be representative for a typical modeling unit (Wang-Erlandsson et al., 2016).

In many model applications, S_r is parameterized with a look-up table approach, attributing the same parameter value to all catchments or cells belonging to the same land-cover class and/or soil type. This approach has the disadvantage of neglecting the variability of rooting properties within one vegetation type. Alternatively, S_r is treated as a tuneable parameter and estimated through calibration, at the expense of interpretability. In addition to those drawbacks, these two approaches treat S_r as a time-invariant parameter. However, rooting properties have been shown to adapt to edaphic and climatic conditions (Gentine et al., 2012), and the inclusion of a dynamic S_r in models has the potential to increase the reliability of projections under a changing climate (Savenije and Hrachowitz, 2017). Several approaches have recently been developed to include the dependence of S_r on environmental conditions. The mass balance approach (de Boer-Euser et al., 2016; Gao et al., 2014) assumes that plants develop their rooting systems so that they can withstand a drought of a certain return period. The storage requirement is estimated based on annual maximal soil moisture deficits over a period of several years, in analogy to engineering calculations used to estimate optimal reservoir size. This approach has been used to generate a global dataset of S_r (Wang-Erlandsson et al., 2016) and has been implemented in a dynamic hydrological model (Nijzink et al., 2016).

Another way to consider the adaptation of vegetation properties is the use of an optimality assumption, i.e. the assumption that vegetation organizes itself in a way that maximizes biological fitness. Eagleson (1982) first introduced optimality principles to ecohydrology, showing their potential in the reduction of model parameterization requirements. Several objective functions have been proposed, such as the minimization of water stress (Eagleson, 1982) or the maximization of net primary productivity (Kleidon and Heimann, 1998). Schymanski et al. (2009) argue that the maximization of net carbon profit –the difference between the amount of carbon assimilated through photosynthesis and the amount used for respiration- is a more appropriate objective function, as the carbon not used for growth and maintenance can be invested into seeds, defense compounds or symbiotic relationships, which all contribute to increase an individual's fitness. Furthermore, this

Hydrol. Earth Syst. Sci. Discuss., https://doi.org/10.5194/hess-2017-723
Manuscript under review for journal Hydrol. Earth Syst. Sci.
Discussion started: 19 December 2017

approach offers a solution to the trade-off between the sometimes conflicting objectives of stress minimization and productivity maximization (Schymanski et al., 2009).

A number of optimality-based approaches have been proposed to estimate Z_e or other rooting properties, such as the shape of the root profile (Guswa, 2008; Yang et al., 2016). Yang et al. (2016) identified the approach proposed by Guswa (2008) as the most meaningful from a hydrological and ecological point of view. This model (see Section 2.1) calculates the optimal rooting depth as the level where the marginal carbon costs of deeper roots starts to outweigh the marginal benefit. Its optimization target is thus similar to the net carbon profit. The model requires an estimation of vegetation properties, as well as long-term climate characteristics. Estimates of Z_e obtained with this approach were used in a hydrological model (Donohue et al., 2012), leading to a higher performance than other parameterizations (Yang et al., 2016). The original version of the model, which has been used in these studies, assumes an intensive water uptake strategy, typical for short-lived vegetation. Guswa (2010) proposed an alternative version of the model, with a water uptake strategy corresponding to the more conservative behavior of trees. While the behavior of both models is similar across most climatic conditions, the rooting depths obtained with the 2010 version are substantially larger than with the 2008 version in energy-limited systems. In this study, we evaluate the potential of the Guswa (2010) approach to parameterize S_r in temperate forests. First, to increase the general applicability of the model, we provide a numerical approximation of its central function (the probabilistic soil moisture model of Porporato et al. (2004)), leading to a much simpler expression. Then, we compare estimates of S_r obtained with this parameterization against S_r values obtained by calibrating a local water balance model against observations of latent heat flux and soil water content at 15 eddy covariance sites of the FLUXNET network (Baldocchi et al., 2001). We also investigate the differences in S_r estimates obtained with the two versions of Guswa's model, as well as the sensitivity of model estimates to root morphological and carbon budget parameters.

2 Methods

2.1 Guswa's optimal rooting depth models

2.1.1 Model concepts

The optimal rooting depth model of Guswa (2008) was developed as a framework to study the effect of climate, soil and vegetation properties on rooting depth. Although its original purpose was to provide process insight, it has been used to generate estimates of Z_e in studies at regional (Donohue et al., 2012; Smettem and Callow, 2014) and global (Yang et al., 2016) scale. The fundamental assumption of the model is that plants develop their rooting systems in a way that maximizes net carbon gain. The model compares the benefits of deeper roots (additional carbon uptake through increased transpiration) with the associated costs (construction and maintenance respiration), and sets the optimal rooting depth at the level where the marginal cost equals the marginal benefit. This is expressed as:

$$\frac{\gamma_r \times D_r}{L_r} = w_{ph} \times f_{seas} \times \frac{d\langle T \rangle}{dZ_e}, \quad (1)$$

Hydrol. Earth Syst. Sci. Discuss., https://doi.org/10.5194/hess-2017-723
Manuscript under review for journal Hydrol. Earth Syst. Sci.
Discussion started: 19 December 2017

Hydrology and Earth System Sciences
Discussions

where γ_r is root respiration rate [mg C g^{-1} roots day^{-1}], D_r root length density [cm roots cm^{-3} soil], L_r specific root length [cm roots g^{-1} roots], w_{ph} photosynthetic water use efficiency [g C cm^{-3} H_2O], f_{seas} growing season length [fraction of a year] and $\langle T \rangle$ mean daily transpiration[mm day^{-1}] during the growing season. The left hand side of Eq. 1 represents the marginal cost of an increase in rooting depth, and the right hand side represents the associated benefit. The last term in Eq. 1 requires the definition of a function relating average transpiration to rooting depth. Guswa (2008) uses the stochastic model of Milly (1993). This model treats precipitation as a Poisson process, characterized by frequency λ [events per day] and average depth α [mm per event]. Such a formulation has been used in many ecohydrological studies at the daily timescale (Porporato et al., 2004; Rodriguez-Iturbe et al., 1999). Transpiration is then expressed as

$$\langle T \rangle = \alpha\lambda \frac{exp[\kappa Z_e/\alpha(1-W)]-1}{exp[\kappa Z_e/\alpha(1-W)]-W}. \quad (2)$$

where κ is the water holding capacity of the soil [mm water depth/mm soil depth] and W the ratio of effective precipitation P_{eff} and potential transpiration T_{pot}. P_{eff} is mean daily precipitation available for transpiration (i.e. minus interception and soil evaporation) and T_{pot} is a hypothetical daily transpiration assuming no soil moisture stress [both in mm day^{-1}]. Substituting Eq. 2 into Eq. 1 and solving for Z_e gives

$$Z_e = \frac{\alpha}{\kappa(1-W)} ln(X), \quad (3)$$

where X is defined as:

$$X = \begin{cases} W\left[1 + \frac{\kappa}{\alpha}\frac{(1-W)^2}{2A} - \sqrt{\frac{\kappa}{\alpha}\frac{(1-W)^2}{A} + \left(\frac{\kappa}{\alpha}\frac{(1-W)^2}{2A}\right)^2}\right] & if\ W > 1 \\ W\left[1 + \frac{\kappa}{\alpha}\frac{(1-W)^2}{2A} + \sqrt{\frac{\kappa}{\alpha}\frac{(1-W)^2}{A} + \left(\frac{\kappa}{\alpha}\frac{(1-W)^2}{2A}\right)^2}\right] & if\ W < 1 \end{cases}, \text{ and} \quad (4)$$

$$A = \frac{\gamma_r \times D_r}{L_r \times w_{ph} \times T_{pot} \times f_{seas}}. \quad (5)$$

For a full derivation of Eqs. 3 to 5, we refer to Guswa (2008).

The transpiration model of Milly (1993) (Eq. 2) assumes that the vegetation transpires at potential rate as long as there is available water in the soil, and that transpiration ceases when the soil moisture reservoir is depleted. This reflects a water uptake strategy typical for many grasses, which tend to maximize carbon assimilation and seed production when water is available, and enter a dormant state or die in drier periods. As long-lived organisms, trees generally have a more conservative water uptake strategy (Chaves, 2002). To examine the effect of water uptake strategy on modeled rooting depth, Guswa (2010) proposed an alternative version of the optimal rooting depth model, where Eq. 2 is replaced with another function, formulated by Porporato et al. (2004):

$$\langle T \rangle = T_{pot} W - \frac{\exp(-Z_n) Z_n^{WZ_n - 1}}{\gamma(WZ_n, Z_n)}, \quad (6)$$

where $\gamma(\cdot,\cdot)$ is the lower incomplete gamma function (Weisstein, n.d.), and Z_n is rooting depth expressed as the number of average precipitation events that can be stored within the rooting zone. Z_n is related to the effective rooting depth Z_e through the following relationship:

Hydrol. Earth Syst. Sci. Discuss., https://doi.org/10.5194/hess-2017-723
Manuscript under review for journal Hydrol. Earth Syst. Sci.
Discussion started: 19 December 2017

$$Z_n = \frac{\kappa Z_e}{\alpha}. \quad (7)$$

This model assumes a linear decrease of transpiration with decreasing soil water content, and reflects the more conservative water uptake strategy of trees.

In both studies, Z_e is at its maximum when water supply and demand are approximately equal. In energy-limited environments, Z_e is more sensitive to changes in rainfall frequency rather than average depth, while the opposite is true under water-limited conditions. The more conservative water-use strategy consistently leads to deeper roots when all parameters are equal, especially under energy-limited conditions. In the rest of this paper, the two versions of Guswa's optimal rooting depth model will be referred to as G08 and G10.

2.1.2 Numerical approximation

Differentiating and rearranging the model of Porporato et al. (2004) (Eq. 6, hereafter referred to as Porporato's equation) leads to rather cumbersome expressions, which limits its practical applicability. Therefore, the Michaelis-Menten equation was used here as an approximation. This equation, widely used in biochemistry to describe the rate of enzymatic reactions, can be written as:

$$\frac{\langle T \rangle}{T_{pot}} \approx \frac{v_m Z_n}{m + Z_n}, \quad (8)$$

where v_m is the upper asymptote and m is the value of Z_n for which $\langle T \rangle / T_{pot}$ is half of v_m. It seems sensible to define v_m as the upper limit of $\langle T \rangle / T_{pot}$, i.e. W in the water-limited case and 1 in the energy-limited case. The parameter m was then adjusted for 28 different values of W (ranging from 0.3 to 3) to maximize the fit with a series of points obtained with Porporato's equation for values of Z_n ranging between 1 and 12. However, curves obtained this way only provided a poor approximation (not shown). More flexibility was given to Eq. 8 by treating v_m as a free parameter as well. While this decreases the interpretability of the Michaelis-Menten parameters, it provides a good fit to the results of Porporato's equation. The resulting curves are shown in Fig. 1 a) for selected values of W.

Hydrol. Earth Syst. Sci. Discuss., https://doi.org/10.5194/hess-2017-723
Manuscript under review for journal Hydrol. Earth Syst. Sci.
Discussion started: 19 December 2017

Hydrology and Earth System Sciences
Discussions
Open Access
EGU

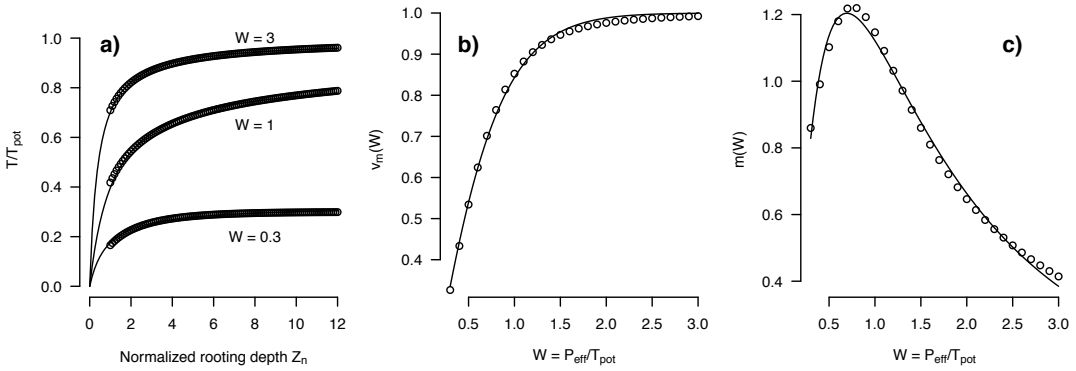

Figure 1: (a) numerical approximation of Porporato's formula (Eq. 6) for three values of the wetness index W. The circles show values calculated with the original formula, and the lines represent Eq. 7, with the parameters $v_m(W)$ and $m(W)$ as calibration parameters. (b) Dependence of the parameter $v_m(W)$ on W. The circles indicate the parameter values obtained for each level of W, and the line shows Eq. 8. (c) Analogous to (b) for the parameter $m(W)$ and Eq. 9.

The values for v_m and m calibrated for each level of W are shown in Fig. 1 b) and c). As these values have been calibrated together, they cannot be directly interpreted in physical terms. However, v_m is always close to the upper limit of $\langle T \rangle / T_{pot}$ (dotted line in Fig. 1 b) and never exceeds 1. Similarly, m, which controls the steepness of the curve, can be related to W. It has a maximum near $W = 1$, suggesting that transpiration is most sensitive to rooting depth when water supply and demand are approximately equal, as noted by Guswa (2008, 2010).

Table 1: Values of the coefficients used to relate the fitted coefficients v_m and m to W in Equations 8 and 9.

Coefficient	Value
k_{v1}	1.851
k_{v2}	1.255
k_{m1}	3.2468
k_{m2}	0.5741
k_{m3}	0.9694

The solid lines in Fig. 1 show the functions selected to estimate v_m and m from W. For v_m, the Janoschek function was chosen:

$$v_m(W) = 1 - exp(-k_{v1} W^{k_{v2}}). \quad (9)$$

Hydrol. Earth Syst. Sci. Discuss., https://doi.org/10.5194/hess-2017-723
Manuscript under review for journal Hydrol. Earth Syst. Sci.
Discussion started: 19 December 2017

The values of the coefficients k used in Eqs. 9 and 10 are given in Table 1. For m, the selected function is based on the PDF of the lognormal distribution:

$$m(W) = k_{m1}\frac{1}{W}\frac{1}{k_{m2}\sqrt{2\pi}}exp\left(-\frac{(ln(W)-k_{m3})^2}{2k_{m2}^2}\right). \quad (10)$$

The relationship of mean transpiration to rooting depth can then be written as:

$$\frac{d\langle T\rangle}{dZ_e} = T_{pot}\frac{\kappa}{\alpha}\frac{v_m(W)m(W)}{(m(W)+Z_n)^2}. \quad (11)$$

By combining Eq. 11 with the original Guswa model (Eq. 1) and solving for Z_n, the optimal normalized rooting depth can be calculated as:

$$Z_n = \sqrt{\frac{f_{seas}\times T_{pot}\times(\kappa/\alpha)\times w_{ph}\times L_r\times v_m(W)\times m(W)}{\gamma_r\times D_r}} - m(W). \quad (12)$$

The optimal effective rooting depth Z_e is calculated as $Z_e = \frac{\alpha}{\kappa}Z_n$, and the corresponding rooting zone storage capacity as $S_{max} = \alpha Z_n$.

2.1.3 Implementation

Unlike in the original model description, this method of calculating S_{max} does not account for the water lost to soil evaporation or understory transpiration. Instead, stand-scale S_r is defined as the sum of overstory S_{max} and a storage volume for understory water use. For temperate forests, one can generally assume that the forest floor is covered with a layer of shrubs or non-woody plants, and that bare soil evaporation is negligible. The storage volume for the understory can then in turn be estimated assuming that its rooting system is optimized, as constrained by the amount of energy reaching the forest floor. Donohue et al. (2012) use a similar approach, by first calculating an optimal rooting depth for both trees and grasses, and providing a grid-cell average by weighting these two values with the respective fractional cover. Their analysis was carried out at a resolution of 0.05°. For smaller spatial units (e.g. a forest stand), however, canopy cover is probably not a good criterion to delimit the rooting zones of trees and grasses. Indeed, as tree rooting systems generally extend far beyond the crown (Kutschera and Lichtenegger, 2002), it is assumed here that the roots of trees cover the whole area, and are in competition with the roots of the understory. As a first approximation, the competition aspect is neglected here, and S_r is calculated as the sum of the optimized storage capacities for the overstory and the understory. Figure 2 shows the structure of a sample forest stand, and the simplifying assumptions made here. Despite their spatial heterogeneity, above- and belowground vegetation and site characteristics are assigned a single value. Partitioning of incoming water and available energy is governed by the leaf area index (LAI) of the overstory.

Hydrol. Earth Syst. Sci. Discuss., https://doi.org/10.5194/hess-2017-723
Manuscript under review for journal Hydrol. Earth Syst. Sci.
Discussion started: 19 December 2017

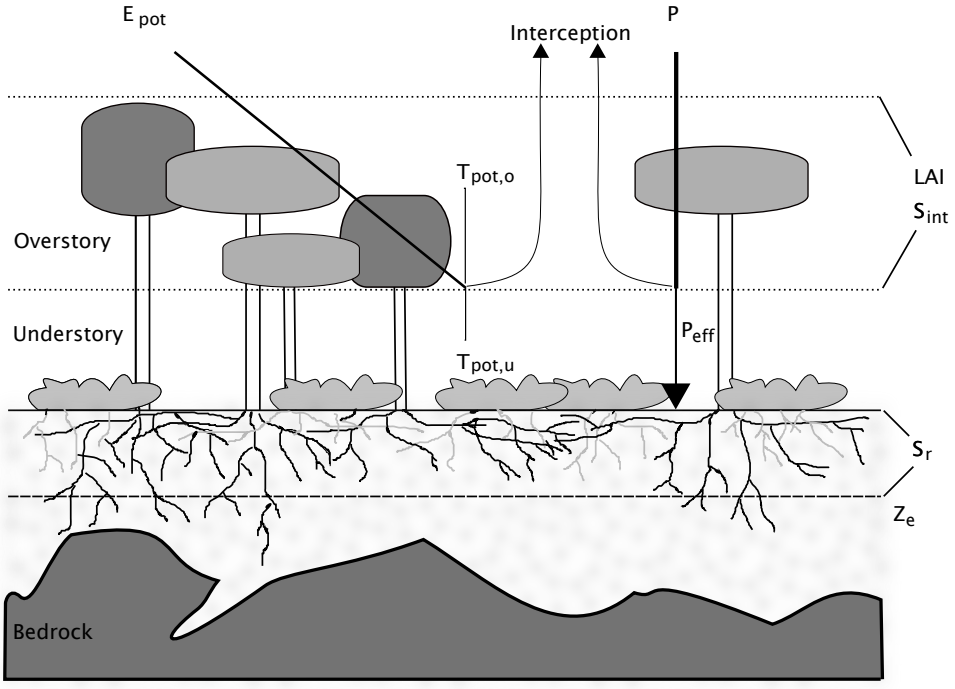

Figure 2: Schematic representation of a forest stand, together with the simplifications used in this study. The stand is heterogeneous in terms of overstory and understory density, as well as soil depth. In the model, both aboveground and belowground properties are integrated to stand-level variables. The crowns of the overstory trees form a canopy described by the variables leaf area index (LAI) and interception storage capacity (S_{int}). LAI determines the partitioning of available energy E_{pot} between potential transpiration of the overstory and understory ($T_{pot,o}$ and $T_{pot,u}$, respectively). Incoming precipitation is divided between effective precipitation reaching the ground P_{eff}, and interception loss. No distinction is made between understory transpiration, understory interception loss and soil evaporation. Below ground, rooting depth is expressed as a stand-scale average (Z_e). Rooting zone water storage capacity S_r is the product of Z_e and soil water holding capacity, assumed to be constant over the whole stand, despite its high horizontal and vertical heterogeneity in reality.

Available energy, represented by mean daily Penman (1948) potential evapotranspiration (E_{pot}), is divided between overstory and understory potential transpiration, $T_{pot,o}$ and $T_{pot,u}$, as follows:

$$T_{pot,o} = E_{pot} \times \left(1 - exp(-k \times LAI)\right) \times 0.75, \text{ and } T_{pot,u} = E_{pot} \times exp(-k \times LAI), \quad (13)$$

where k is the canopy light extinction coefficient, taken as 0.5, and LAI is overstory leaf area index during the growing season. The factor 0.75 in Eq. 13 accounts for the energy used for interception evaporation and for stomatal and aerodynamic resistances, and was set based on the meta-analysis of Granier et al. (1999). As soil and understory evaporation are mainly

determined by the amount of energy reaching the forest floor (Granier et al., 1999), these processes are lumped together. As overstory and understory share the same soil moisture reservoir, the wetness indices W_o and W_u are calculated as follows:

$W_o = P_{eff}/T_{pot,o}$, and $W_u = P_{eff}/T_{pot,u}$. (14)

The storage capacity for the overstory is calculated using Eq. 12 (G10 model), and the value for the understory is calculated using Eqs. 2 to 5 (G08 model):

$S_r = G10(T_{pot,o}, W_o, \alpha, \kappa, V_{tree}) + G08(T_{pot,u}, W_u, \alpha, \kappa, V_{grass})$, (15)

where V_{tree} and V_{grass} are the vegetation parameter sets for trees and grass, given in Table 2 (see also Section 2.1.4 below).

Table 2: Values of the vegetation parameters needed for the optimal rooting depth model, as compiled by (Donohue et al., 2012).

Parameter	Trees	Grass
w_{ph} [mmol CO_2 cm^{-3} water]	0.33	0.22
$\gamma_{r,20}$ [mmol CO_2 g^{-1} roots day^{-1}]	0.5	0.5
L_r [cm roots g^{-1} roots]	1500	1500
D_r [cm roots cm^{-3} soil]	0.1	0.1

2.1.4 Parameterization

In the present study, the climate parameters are derived from daily averaged measurements of air temperature, precipitation, vapor pressure deficit (VPD), global radiation and wind speed at 15 FLUXNET sites (see Section 2.2.1 below). To define the start of the growing season, the species-specific spring phenology model developed and parameterized by Kramer (1996) was applied at each site, with the parameters corresponding to the dominant species. Following Zierl (2001), the onset of leaf senescence in autumn was set to the first time the four-day mean temperature drops below 5°C. The end of the growing season is set to 14 days after the onset of leaf senescence. For *Pinus pinaster*, for which no species-specific parameters were available, the growing season was assumed to last from April to October. Potential evapotranspiration was calculated using the Penman (1948) equation and averaged to mean daily values over the growing season. To calculate precipitation frequency λ and average depth α, a precipitation event was defined as a period of one or more consecutive days with precipitation greater than 0.5 mm/day. Effective precipitation P_{eff} was estimated as follows (Guswa, 2008):

$P_{eff} = \alpha\lambda \times exp(-S_{int}/\alpha)$, (16)

where S_{int} is the canopy interception storage capacity [mm]. This value was estimated from LAI using the relationship proposed by Menzel (1997) and Vegas Galdos et al. (2012):

$S_{int} = k_{int} \times log_{10}(1 + LAI)$, (17)

where k_{int} is an empirical parameter, set to 1.6 for broadleaved forests, 1.8 for mixed forests and 2 for coniferous forests (Vegas–Galdos et al., 2012).

The vegetation parameters were taken from Donohue et al. (2012), who compiled them from values found in the literature. The parameter values for trees and grass are shown in Table 2. Root respiration rate is parameterized as a function of temperature, following Yang et al. (2016):

$$\gamma_r = \gamma_{r,20} Q_{10}^{\left(\frac{T-20}{10}\right)}, \quad (18)$$

where T is the mean soil temperature over the growing season, and Q_{10} is a coefficient indicating the effect of a 10 K rise in temperature. In the absence of soil temperature measurements, air temperature can be taken as a proxy (Yang et al., 2016). Based on the experimental findings of Keller (1967), Q_{10} was set to 2.

This parameter set reflects the range of values reported in the literature for trees. However, these values have been shown to vary across species. For example, the root morphological parameters differ between broadleaves and conifers, with a markedly higher specific root length L_r, and a tendency towards higher root length density D_r, in the former (Kalliokoski et al., 2010; Withington et al., 2006). The variables related to the plant's carbon budget can also be expected to vary across species groups. Typically, species with a high degree of shade tolerance tend to have a higher water-use efficiency and lower respiration rates, and vice-versa (Polster, 1950; Valladares and Niinemets, 2008). The sites selected for this study (see Section 2.2.1 below) include both broadleaved and conifer stands, as well as sites dominated by shade tolerant (*Abies alba, Fagus sylvatica*), intermediate (*Picea abies, Quercus cerris*) and intolerant species (*Pinus sylvestris, P. pinaster*). The potential of including species-specific parameterizations was assessed by varying the ratios L_r/D_r and $w_{ph}/\gamma_{r,20}$ within plausible ranges. Assuming that the generic parameterization of Donohue et al. (2012) represents intermediate conditions, the ratio L_r/D_r (15'000 in the original parameterization) was varied between 10'000 and 15'000 for conifers, and between 15'000 and 20'000 for broadleaves. The ratio $w_{ph}/\gamma_{r,20}$ (0.66) was increased or reduced by up to 15% for shade tolerant and intolerant species, respectively.

2.2 S_r estimated through model calibration

As mentioned above, S_r and Z_e are model parameters that cannot be directly measured in the field. Due to the high spatial heterogeneity of rooting depth and soil properties, field measurements of rooting depth are not necessarily indicative of the average conditions in a forest stand. An alternative to measurements is the estimation of parameter values through model calibration (Gao et al., 2014). In this study, $S_r$was estimated at 15 eddy covariance sites from the FLUXNET network (Baldocchi et al., 2001) by calibrating the local water balance model FORHYTM (Forest Hydrology Toy Model; Speich et al. (under review); see https://github.com/mspeich/forhytm). Modeled total evaporation (E_{tot}, defined as the sum of canopy transpiration, soil and understory evaporation and interception loss) and relative extractable water (REW; see below) were compared against measurements at half-hourly time steps.

Hydrol. Earth Syst. Sci. Discuss., https://doi.org/10.5194/hess-2017-723
Manuscript under review for journal Hydrol. Earth Syst. Sci.
Discussion started: 19 December 2017

Hydrology and Earth System Sciences
Discussions
Open Access
EGU

2.2.1 FLUXNET site selection

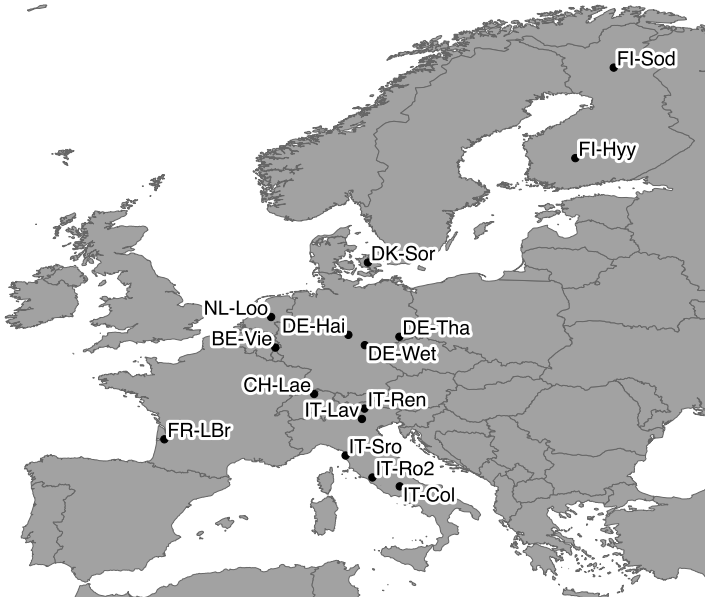

Figure 3: Map of the 15 FLUXNET sites used in this study. Base map elements from Natural Earth.

Table 3 gives an overview of the FLUXNET sites used in this analysis, and their location is shown on Fig. 3. The conditions for site selection were the following: (1) at least four years of continuous latent heat flux measurements in the FLUXNET-2015 (Tier 1) or La Thuile (fair use) datasets; (2) belonging to a forested IGBP land cover class (either Evergreen Needleleaf Forest (ENF), Evergreen Broadleaf Forest (ENF), Deciduous Broadleaf Forest (DBF), Deciduous Needleleaf Forest (DNF) or Mixed Forest (MF)); (3) temperate or cold climate (group C or D in the Köppen-Geiger (Köppen, 2011) classification); (4) no a priori indications (e.g. in the site description) of a shallow water table or irrigation; (5) availability of soil water content (SWC) measurements at a depth that can be taken as representative for the average conditions in the rooting zone. The last criterion greatly limits the number of sites retained in this analysis, as for many sites, the soil water measurements are representative for the near-surface conditions only. It is however necessary to exclude these sites, as the absolute values and dynamics of soil moisture in the uppermost layers can differ greatly from the conditions at greater depths (Miller et al., 2007). For each site, the suitability of SWC measurements was determined through a subjective assessment of the SWC curves. The soil moisture content at field capacity θ_{FC} was estimated by eye as the level where SWC stabilizes after a refilling event, and the soil moisture content at the wilting point θ_{WP} was assumed to correspond to the lowest SWC

Hydrol. Earth Syst. Sci. Discuss., https://doi.org/10.5194/hess-2017-723
Manuscript under review for journal Hydrol. Earth Syst. Sci.
Discussion started: 19 December 2017

Hydrology and Earth System Sciences
Discussions

measured over the whole period. The corresponding soil water holding capacity κ, i.e. the difference between θ_{FC} and θ_{WP}, is reported in Table 3.

Table 3: Overview of the FLUXNET sites used in this study. Where a model validation was performed, the validation period is given in brackets.

Site	Years used	Lat/Lon	m asl	Dominant species	LAI	f_c	κ [mm/mm]	Reference
Vielsalm (BE-Vie)	1997-2008 (2010-2012)	50.3, 6	491	Fagus sylvatica	4.5	0.9	0.11	Aubinet et al. (2001)
Lägeren (CH-Lae)	2005-2010 (2011-2013)	47.45, 8.4	689	Fagus sylvatica,	5.5	0.9	0.12	Etzold et al. (2011)
Hainich (DE-Hai)	2004-2009 (2000-2003)	51.1, 10.5	430	Fagus sylvatica	5	0.9	0.28	Anthoni et al. (2004)
Tharandt (DE-Tha)	1997-2003 (2004-2008)	51, 13.6	320	Picea abies	7.2	0.9	0.15	Grünwald and Bernhofer (2007)
Wetzstein (DE-Wet)	2003-2006	50.5, 11.5	703	Picea abies	4	0.9	0.19	Anthoni et al. (2004)
Sorø (DK-Sor)	2008-2013 (2005-2006)	55.5, 11.6	40	Fagus sylvatica	5	0.9	0.19	Wang et al. (2005)
Hyytiälä (FI-Hyy)	2003-2007 (2008-2013)	61.8, 24.3	181	Pinus sylvestris	3.3	0.45	0.3	Lindroth et al. (2008)
Sodankylä (FI-Sod)	2001-2006 (2007-2010)	67.4, 26.6	188	Pinus sylvestris	1.7	0.45	0.06	Lindroth et al. (2008)
Le Bray (FR-LBr)	2003-2008 (2010-2012)	44.7, -0.8	62	Pinus pinaster	2.8	0.8	0.11	Loustau et al. (2005)
Collelongo (IT-Col)	2007-2012 (1997-2001)	41.8, 13.6	1560	Fagus sylvatica	4.5	0.8	0.17	Valentini et al. (1996)
Lavarone (IT-Lav)	2004-2010 (2011-2014)	46, 11.3	1305	Abies alba	9.6	0.9	0.25	Cescatti and Marcolla (2004)
Renon (IT-Ren)	2005-2009 (2010-2013)	46.6, 11.4	1794	Picea abies	5.5	0.9	0.23	Cescatti and Marcolla (2004)
Roccarespam-	2003-2008	42.4,	160	Quercus	4.5	0.9	0.14	Chiti et al. (2010)

Hydrol. Earth Syst. Sci. Discuss., https://doi.org/10.5194/hess-2017-723
Manuscript under review for journal Hydrol. Earth Syst. Sci.
Discussion started: 19 December 2017

pani 2 (IT-Ro2)	(2010-2012)	11.9		cerris				
San Rossore (IT-SRo)	2000-2006 (2007-2009)	43.7, 10.3	6	Pinus pinaster	2.8	0.5	0.06	Chiti et al. (2010)
Loobos (NL-Loo)	1997-2007 (2008-2013)	52.2, 5.7	25	Pinus sylvestris	3	0.8	0.05	Kramer et al. (2002)

2.2.2 Model calibration and parameter estimation

The local water balance FORHYTM was calibrated at each site to obtain estimates of S_r. This model consists essentially of a coupling between the dual-source transpiration and soil evaporation routine of Guan and Wilson (2009) and a soil water balance routine widely used in semi-conceptual hydrological models (Bergström, 1992; Zappa and Gurtz, 2003). Figure 4 a) gives an overview of the water fluxes simulated in FORHYTM. The scheme of Guan and Wilson (2009) assumes an interaction between the energy fluxes between overstory and understory, while accounting for the difference in evaporation between inter-canopy and sub-canopy understory parts. In this routine, available energy, represented by net radiation, is partitioned between overstory and understory/soil using Beer's law (see Eq. 13). Potential transpiration and soil evaporation are then calculated using Penman-Monteith-type equations and scaled according to fractional canopy cover. Incoming precipitation first fills an interception reservoir, whose size (S_{int}) is related to LAI through an empirical relationship proposed by Menzel (1997) and Vegas Galdos et al. (2012) (see Eq. 18).

Hydrol. Earth Syst. Sci. Discuss., https://doi.org/10.5194/hess-2017-723
Manuscript under review for journal Hydrol. Earth Syst. Sci.
Discussion started: 19 December 2017

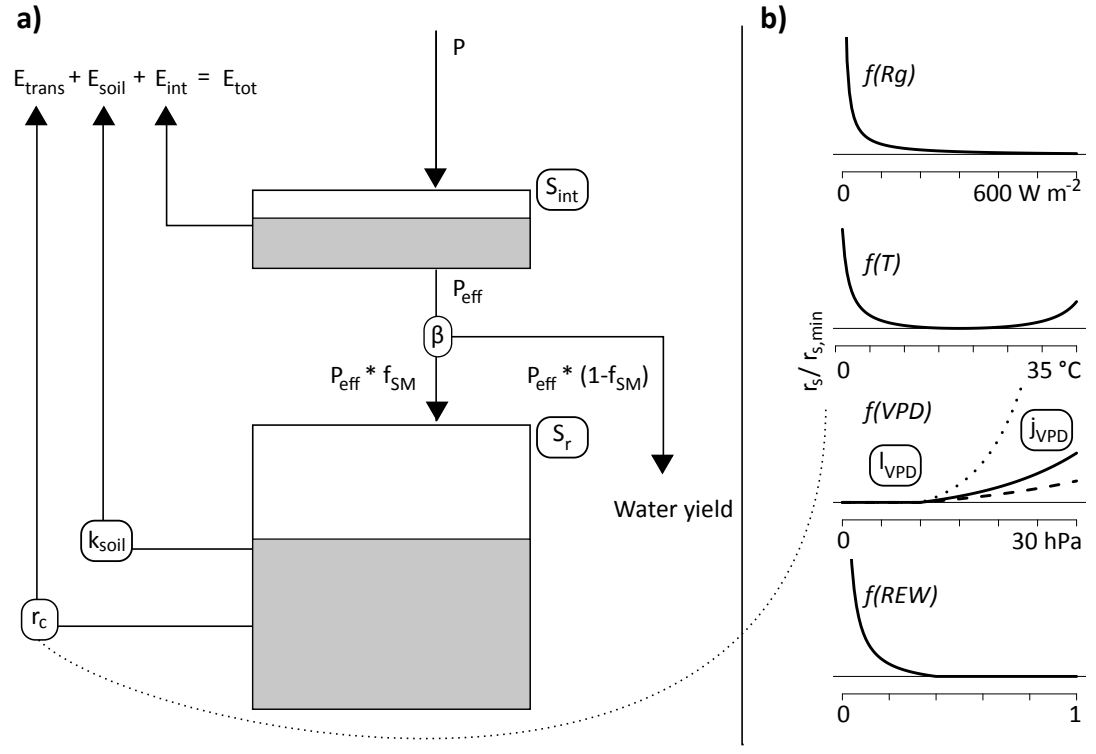

Figure 4: (a) Schematic representation of the water fluxes in the local water balance model FORHYTM. Incoming precipitation P first fills a canopy interception reservoir of size S_{int}, from which water evaporates back to the atmosphere. Precipitation reaching the ground, P_{eff}, is split between the rooting zone storage and runoff/groundwater recharge as a function of the parameter β and the current filling status of the rooting zone storage. This storage is depleted by soil evaporation and overstory transpiration. Soil evaporation is reduced from its potential value as a function of time since the last rainfall and the parameter k_{soil}. Transpiration is controlled by the canopy resistance r_c, i.e. stomatal resistance divided by LAI. (b) Relative increase of stomatal resistance as a function of radiation, air temperature, VPD and REW. When all functions are equal to one (optimal conditions), stomatal resistance is equal to $r_{s,min}$.

A fraction f_{SM} of the water reaching the ground is added to the plant-available soil moisture reservoir S_{SM} as a function of its current filling state and a shape parameter, termed β:

$$f_{SM} = \left(\frac{S_{SM}}{S_r}\right)^{\beta}. \quad (19)$$

The remaining fraction of incoming water $(1 - f_{SM})$ is assumed to leave the system as fast runoff or groundwater recharge, and is not considered further in the model. The reservoir S_{SM} is depleted by canopy transpiration and soil/understory evaporation. The former is controlled by canopy resistance, modeled using a Jarvis-type routine (Jarvis, 1976), whereas the

latter is reduced exponentially from its potential value as a function of the number of days without rain (Morillas et al., 2013). The canopy resistance parameterization uses a multiplicative approach, where a minimum stomatal resistance $r_{s,min}$ [s m^{-1}] is multiplied with several functions of environmental factors (radiation, temperature, VPD and soil moisture; see Fig. 4 b)). As long as these factors are not limiting, the corresponding response function has a value of one. The response functions are greater than one (i.e. the resistance is increased) when the corresponding environmental factor has a sub-optimal value. The response functions for radiation, temperature and soil moisture are parameterized following Stewart (1988). For VPD, the model version used here assumes an exponential reduction of stomatal conductance (the inverse of resistance) with increasing VPD. Furthermore, as not all tree species respond to low VPD values, an additional parameter l_{vpd} [hPa] was introduced, indicating the VPD value above which canopy resistance is affected. The response function for VPD is thus defined as:

$$f_{VPD} = \begin{cases} 1; VPD < l_{VPD} \\ 1/exp\left(j_{VPD} \times (VPD - l_{VPD})\right)\ otherwise \end{cases} \quad (20)$$

Stomatal resistance is then scaled up to canopy scale by dividing by LAI. All calibration parameters of FORHYTM are listed in Table 4. The model also includes a parsimonious snow routine, implemented following Bergström (1992).

All meteorological variables (precipitation, air temperature, VPD, global radiation and wind speed) needed to run FORHYTM are measured at the FLUXNET sites and included in the dataset. The annual maximal leaf area index (LAI) is specified for each site based on literature values (see Table 3). For stands with deciduous species, annual phenology is simulated as described above in Section 2.1.4. Site-specific fractional canopy cover was taken from the site description or estimated based on satellite images on Google Earth.

Table 4: Ranges of the calibration parameters used in this study.

Parameter	Units	Meaning	Minimum	Maximum
S_r	mm	Size of the plant-available soil moisture reservoir	30	500
β	-	Shape coefficient of the soil moisture recharge function	1	6
$r_{s,min}$	s m^{-1}	Minimum stomatal resistance	120	1000
k_{soil}	days	e-folding time of the soil evaporation reduction function	5	30
j_{vpd}	-	Exponent of the VPD-induced reduction of stomatal conductance	-0.18	-0.05
l_{vpd}	hPa	Threshold for stomatal response to VPD	0	20
k_{int}	mm	Link between interception storage and LAI	1.5	4.5

Modeled total evaporation (E_{tot}) and soil moisture were compared against measurements of latent heat flux and soil water content (SWC). SWC measurements were converted to relative extractable water (Granier et al., 2007) as follows:

$$REW = min\left(1, \frac{\theta - \theta_{WP}}{\theta_{FC} - \theta_{WP}}\right). \quad (21)$$

For both outputs, the goodness-of-fit measure is the Kling-Gupta efficiency KGE (Gupta et al., 2009) with the slight modification proposed by Kling et al. (2012). KGE is defined as:

$$KGE = 1 - \sqrt{(r-1)^2 + (\beta - 1)^2 + (\gamma - 1)^2}, \quad (22)$$

where r is the Pearson correlation coefficient between the simulated and observed values, β the bias ratio (ratio of the means of the simulated and observed values), and γ the variability ratio (ratio of the coefficients of variation of the simulated and observed values). The final criterion used to determine the goodness-of-fit, KGE_{AVG}, is the average of the KGE values obtained for TE and REW. Only the time steps that are part of the growing season (given by the phenology model) were considered. Furthermore, time steps where the quality control flag indicated unreliable observations were excluded.

FORHYTM was run at each site with 1000 different combinations of parameter values, sampled from the parameter space given in Table 4 using the Latin Hypercube Sampling procedure of Beachkofski and Grandhi (2002). At each site, the parameter sets with KGE_{AVG} scores equal or greater than the 95th percentile were retained for model validation. Table 3 indicates the calibration and validation periods at each site. Where soil water content measurements were available for the calibration period only, validation was only performed against E_{tot}. Furthermore, as only five years of measurements are available for Wetzstein, no validation was undertaken for that site. The S_r value taken as representative for the site is the median of the S_r of the retained parameter sets.

3 Results

3.1 Calibration and validation of the water balance model FORHYTM

Table 5 shows the KGE scores obtained at each site. The KGE_{evap} values in the validation period range from 0.46 to 0.87, and the KGE_{REW} scores range from 0.12 to 0.83. The lowest scores for evaporation were obtained at the Mediterranean sites Roccarespampani and San Rossore, as well as at the montane-Mediterranean site Collelongo. For Collelongo, the bias component of the KGE_{evap} is consistently greater than one in all validation runs (not shown), indicating that the relatively low score at this site is primarily due to a systematic overestimation of E_{tot}. The lowest KGE_{REW} was obtained at Loobos (0.12). This site also shows a great uncertainty regarding the value of the optimal S_r, as indicated by the large standard deviation. FORHYTM also performed poorly at Roccarespampani, with a KGE_{REW} of 0.32. The calibrated S_r values cover almost the whole parameter range defined in this study and range from 95 (Sodankylä, Renon) to 417 mm (Roccarespampani).

Hydrol. Earth Syst. Sci. Discuss., https://doi.org/10.5194/hess-2017-723
Manuscript under review for journal Hydrol. Earth Syst. Sci.
Discussion started: 19 December 2017

Hydrology and Earth System Sciences
Discussions

Table 5: KGE scores obtained at each site for calibration (first number) and validation (second number). The S_r value is the median of the parameter value in the simulations with KGE_{AVG} equal or greater than the 95th percentile. The value in parentheses is the standard deviation these parameter values. The values obtained with the optimality-based models are shown in the last two columns.

Site	Highest KGE_{evap}	Highest KGE_{REW}	Highest KGE_{AVG}	Calibrated S_r [mm] (SD)	Guswa (2008) S_r	Guswa (2010) S_r
Vielsalm	0.75 / 0.87	0.88 / -	0.8 / -	184 (46)	114	149
Lägeren	0.77 / 0.75	0.74 / 0.69	0.75 / 0.72	185 (52)	122	172
Hainich	0.8 / 0.8	0.58 / -	0.67 / -	267 (50)	237	246
Tharandt	0.82 / 0.77	0.75 / 0.72	0.78 / 0.74	179 (45)	173	178
Wetzstein	0.75 / -	0.73 / -	0.72 / -	164 (58)	207	202
Sorø	0.76 / 0.76	0.78 / 0.79	0.76 / 0.77	249 (59)	190	216
Hyytiälä	0.81 / 0.86	0.8 / 0.68	0.78 / 0.77	246 (53)	148	203
Sodankylä	0.74 / 0.66	0.68 / 0.51	0.68 / 0.58	94 (30)	63	72
Le Bray	0.83 / 0.75	0.78 / -	0.79 / -	272 (61)	168	180
Collelongo	0.85 / 0.55	0.89 / -	0.86 / -	372 (60)	175	225
Lavarone	0.7 / 0.77	0.68 / 0.57	0.68 / 0.67	315 (57)	138	273
Renon	0.81 / 0.78	0.41 / 0.73	0.6 / 0.75	94 (31)	132	218
Roccarespampani	0.73 / 0.46	0.66 / 0.32	0.62 / 0.39	417 (54)	137	183
San Rossore	0.8 / 0.58	0.62 / 0.83	0.58 / 0.71	374 (77)	138	140
Loobos	0.84 / 0.75	0.63 / 0.12	0.71 / 0.44	224 (89)	77	88

Figure 5 a) shows the KGE_{AVG} scores obtained during calibration at Tharandt, plotted against the S_r parameter values (figures analogous to Fig. 5 for all other sites are provided as supplementary material). The highest scores are obtained only for a relatively narrow range of S_r. The time series of the validation runs at Tharandt are shown on Fig. 5 b) for E_{tot} and c) for REW. The observations are plotted against the bounds given by the 5th and 95th percentile of the validation runs. For E_{tot}, the observations are often close to the lower bound, which indicates a tendency of the model to overestimate E_{tot} at this site. The figure further indicates that the model cannot fully capture the interannual variability, as shown by the overestimation of E_{tot} and of REW in 2006. Another source of disagreement between model and observations is the apparent quick refilling of soil moisture after precipitation events, which is not always reproduced by FORHYTM.

Hydrol. Earth Syst. Sci. Discuss., https://doi.org/10.5194/hess-2017-723
Manuscript under review for journal Hydrol. Earth Syst. Sci.
Discussion started: 19 December 2017

Hydrology and Earth System Sciences
Discussions

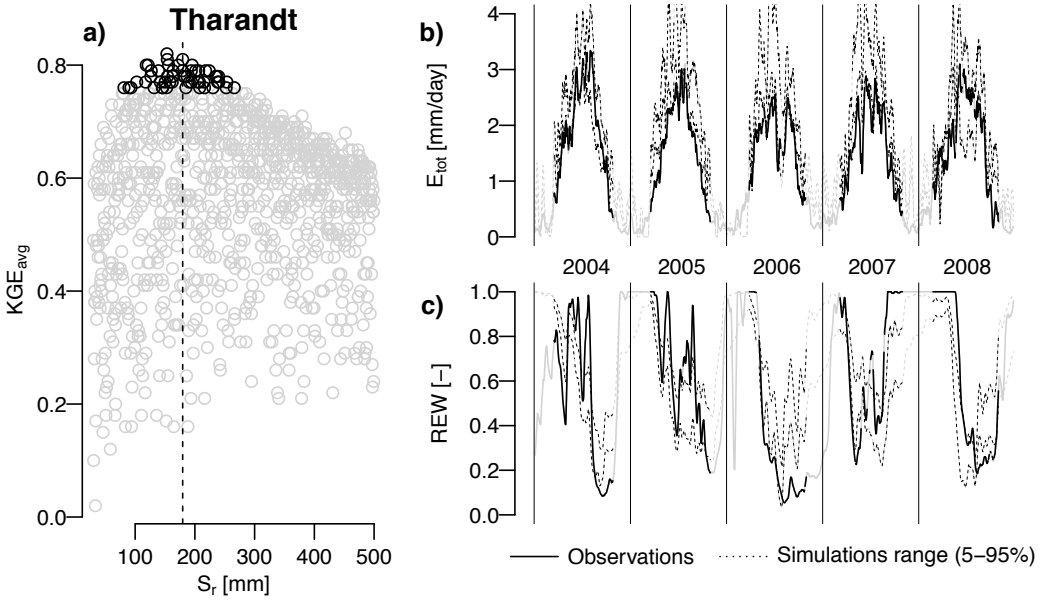

Figure 5: (a) Relationship of the KGE_{avg} obtained during calibration and the parameter values of S_r at Tharandt (calibration period: 1997-2003). The black points have a KGE_{avg} greater or equal to the 95th percentile at this site, and the line shows the median of these values (i.e. the value reported in Table 5). The shape of the relationship shows that KGE_{avg} is quite sensitive to S_r, and there is a relatively narrow range of S_r leading to Pareto-optimal scores. (b) Time series of total evaporation E_{tot} for the validation period (2004-2008) at Tharandt, comparing the observations with simulations conducted using the optimal parameter sets. The solid line shows the observations, and the dotted lines show the 5 and 95% quantiles of the simulations at each time step. For clarity, the time series are presented here as ten-day moving averages, while the simulations were done with a half-hourly time step. (c) Analogous to b), for relative extractable water (REW).

3.2 Climate characteristics of the selected FLUXNET sites

The climate parameters calculated over the calibration period are shown in Table 6. As can be seen on Fig. 6 a), E_{pot} is greater or approximately equal to P during the growing season at most sites. The high montane sites Lavarone and Renon, as well as the montane site Lägeren, are the only sites where precipitation is clearly greater than E_{pot}. Other clusters are formed by the boreal sites, with low E_{pot} and low P; the Mediterranean sites and Le Bray, with high E_{pot} and low P; and the temperate lowland sites, with low E_{pot} and intermediate P. Figure 6 b) shows the distribution of the rainfall properties λ (frequency of events) and α (mean depth). Again, the sites located in the Alps and nearby form a cluster, with a high mean precipitation intensity and an intermediate frequency. The Mediterranean sites are characterized by an intermediate α and

Hydrol. Earth Syst. Sci. Discuss., https://doi.org/10.5194/hess-2017-723
Manuscript under review for journal Hydrol. Earth Syst. Sci.
Discussion started: 19 December 2017

Hydrology and Earth System Sciences
Discussions
Open Access
EGU

low λ, whereas the boreal sites receive precipitation at a high frequency but with a low mean intensity. The temperate lowland sites cover the space between low and intermediate α, and between intermediate and high λ.

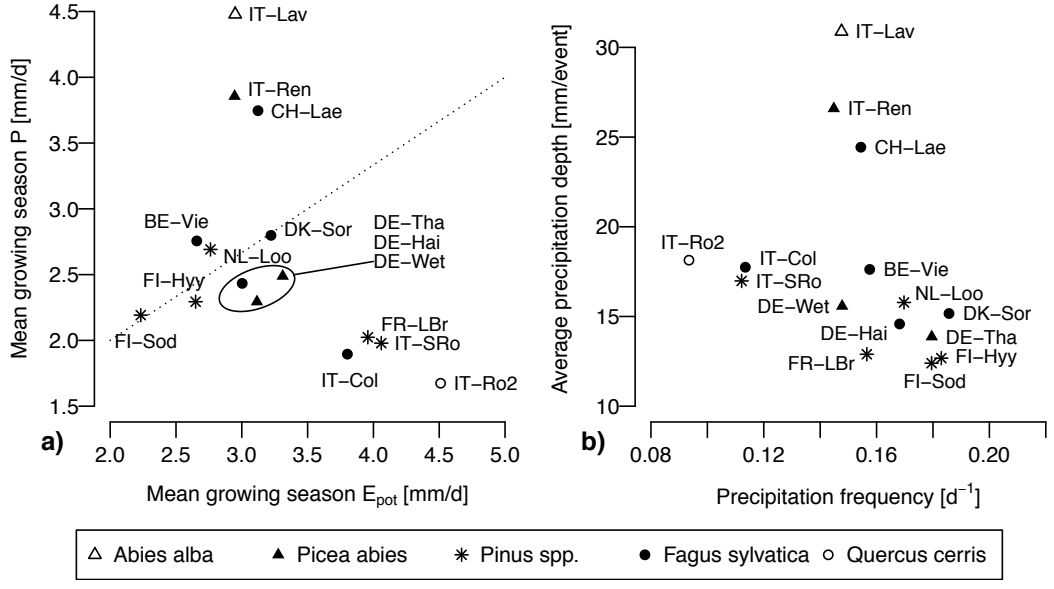

Figure 6: (a) Position of the 15 selected FLUXNET stations in the E_{pot}-P space. The values are daily averages, calculated over the growing seasons of the calibration period. The dotted line is the 1:1 line. Since only the growing season is considered, $E_{pot} > P$ at most sites. (b) Position of the sites in the λ-α space.

Table 6: Climate parameters, calculated as growing-season averages over the calibration period (see text).

Site	P [mm/d]	P_{eff} [mm/d]	λ [1/d]	α [mm]	E_{pot} [mm/d]	$T_{pot,o}$ [mm/d]	$T_{pot,u}$ [mm/d]	f_{seas}
Vielsalm	2.76	2.55	0.16	17.62	2.66	1.78	0.28	0.47
Lägeren	3.74	3.53	0.15	24.43	3.12	2.2	0.2	0.47
Hainich	2.43	2.23	0.17	14.58	3	2.07	0.25	0.48
Tharandt	2.48	2.18	0.18	13.87	3.31	2.42	0.09	0.45
Wetzstein	2.29	2.1	0.15	15.58	3.12	2.02	0.42	0.4
Sorø	2.8	2.58	0.19	15.16	3.22	2.23	0.25	0.47

Hydrol. Earth Syst. Sci. Discuss., https://doi.org/10.5194/hess-2017-723
Manuscript under review for journal Hydrol. Earth Syst. Sci.
Discussion started: 19 December 2017

Hyytiälä	2.29	2.08	0.18	12.67	2.65	1.61	0.51	0.38
Sodankylä	2.19	2.04	0.18	12.39	2.23	0.96	0.95	0.28
Le Bray	2.02	1.85	0.16	12.9	3.96	2.24	0.98	0.59
Collelongo	1.89	1.77	0.11	17.74	3.8	2.55	0.4	0.42
Lavarone	4.48	4.19	0.15	30.88	2.95	2.19	0.02	0.38
Renon	3.85	3.62	0.14	26.58	2.95	2.06	0.19	0.31
Roccarespampani	1.67	1.57	0.09	18.13	4.51	3.02	0.48	0.52
San Rossore	1.98	1.85	0.11	16.98	4.06	2.29	1	0.59
Loobos	2.69	2.49	0.17	15.78	2.76	1.61	0.62	0.48

3.3 S_r parameterization

The S_r estimates obtained with the G08 and G10 models are given in the two last columns of Table 5. Figure 7 a) and b) show these estimates plotted against the calibration-based S_r. The horizontal bars indicate the standard deviation of the calibrated values, as given in Table 5. In these two plots, the parameterization of Donohue et al. (2012) was used. Some sites show a good agreement between the two methods in both cases, such as the boreal pine sites Hyytiälä and Sodankylä, and the beech sites Sorø and Hainich. On the other hand, some sites show a strong disagreement in both cases. The optimality-based S_r are much lower than the calibrated value at the Mediterranean sites Roccarespampani and San Rossore (and, to a lesser extent, Collelongo), and at the temperate pine sites Loobos and Le Bray, and are much higher at the high-elevation spruce site Renon. The results of G08 and G10 are broadly similar, but with some notable exceptions. G10 gives much higher estimates than G08 (by 90 to 140 mm) for the high-elevation sites Lavarone (fir) and Renon (spruce), and somewhat higher estimates (by 30 to 50 mm) for the beech sites Vielsalm and Lägeren. In the case of Lavarone, Vielsalm and Lägeren, the G10 estimates are much closer to the calibrated values. For Renon, the optimality-based value is much higher than the calibrated value in both cases, but the G10 estimate is much further from the calibrated value than the G08 estimate.

Hydrol. Earth Syst. Sci. Discuss., https://doi.org/10.5194/hess-2017-723
Manuscript under review for journal Hydrol. Earth Syst. Sci.
Discussion started: 19 December 2017

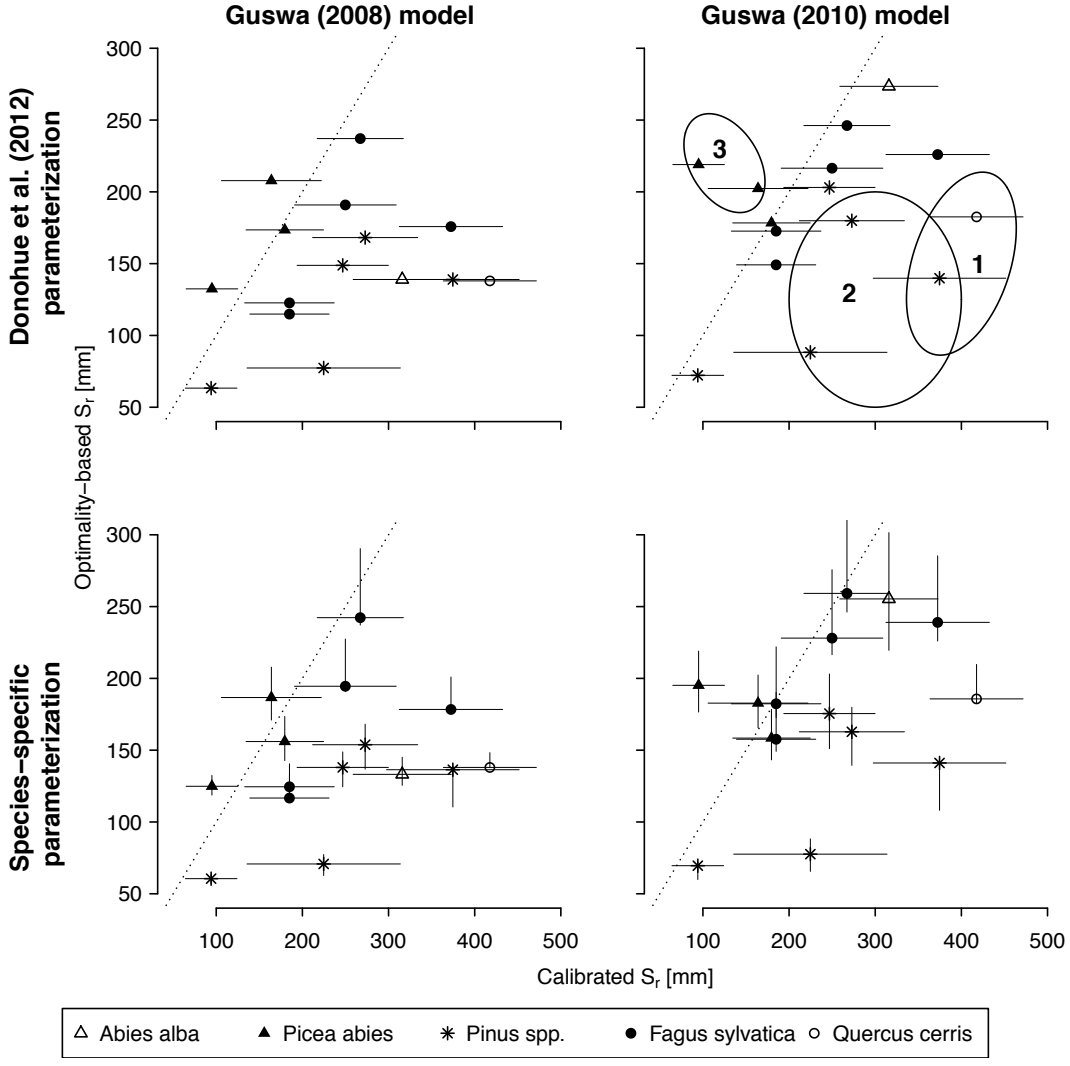

Figure 7: (a) and (b) Results of the optimality-based S_r estimates obtained with G08 and G10, respectively, plotted against the calibration-based S_r. The horizontal bars show the standard deviation of the calibrated S_r at each site. For these figures, the generic parameterization of Donohue et al. (2012) was applied. The ellipses on b) show the cases with strong mismatches between G10 and calibrated S_r, discussed in section 4.2: Mediterranean climates (1), pine sites on sandy soils (2), and spruce sites along an elevational gradient (3). (c) and (d) Same as above, but with the vegetation parameters modified as described in Section 2.1.4. The points show the results obtained by reducing the L_r/D_r ratio by 20% for conifer stands, and by increasing or reducing the

Hydrol. Earth Syst. Sci. Discuss., https://doi.org/10.5194/hess-2017-723
Manuscript under review for journal Hydrol. Earth Syst. Sci.
Discussion started: 19 December 2017

$w_{ph}/\gamma_{r,20}$ ratio by 5% for shade tolerant and intolerant species, respectively. The vertical bars show the ranges of values obtained by varying L_r/D_r by up to 33% and $w_{ph}/\gamma_{r,20}$ by up to 15%.

Figure 7 c) and d) illustrate the effect of varying the vegetation parameters. The points show the results obtained by setting the ratio L_r/D_r to 12'000 for conifers, and by increasing or decreasing the ratio $w_{ph}/\gamma_{r,20}$ by 5% for shade tolerant and intolerant species, respectively. The vertical bars indicate the whole range of values obtained by varying the vegetation parameters as described in Section 2.1.4. The possible ranges are up to 100 mm, and the sensitivity of S_r to vegetation parameters is greater for larger S_r estimates.

4 Discussion

4.1 Suitability of the S_r concept

The goodness-of-fit scores obtained by FORHYTM during validation give an indication of the reliability of the calibrated S_r estimates and, more generally, on the suitability of this model structure to simulate local water balance under various conditions. For comparison, Chaney et al. (2016), who also calibrated an evapotranspiration routine against half-hourly eddy covariance data using KGE, obtained a median score of 0.73 after parameter optimization. Sprenger et al. (2015) obtained KGE scores ranging from 0.43 to 0.8 for soil moisture time series. The scores obtained here for E_{tot} range from 0.66 to 0.87 for temperate and boreal sites, and from 0.46 to 0.58 at Mediterranean sites. For the REW time series, the sites with scores below the range cited above are Roccarespampani and Loobos. These results suggest that FORHYTM is able to reproduce the local water balance at most temperate and boreal sites, but that its predictive ability is limited under Mediterranean conditions. By extension, this gives confidence that the calibrated S_r are representative for the actual site conditions, at least at the temperate and boreal sites. Under Mediterranean conditions, transpiration may be more sensitive to the vertical distribution of soil moisture and roots (Bai et al., 2017). Therefore, the use of a bulk S_r neglecting vertical root distribution may not be appropriate at those sites. An exception within the temperate sites is Loobos, where the performance of FORHYTM for REW was worst (0.12). A particularity of this site is that it is located on a sand dune, i.e. on a deep soil with very low water holding capacity. Under these conditions, the concept of a rooting zone storage capacity, i.e. a clearly defined volume of soil where water can be accessed by the roots, may not be applicable.

At the high-elevation Mediterranean site Collelongo, the relatively low performance during the validation period contrasts with the high calibration efficiency. At this site, the calibration and validation periods (2007-2012 and 1997-2001, respectively) were not immediately contiguous. The disappointing performance in the validation period might therefore be due to changing conditions between the two periods. Indeed, the validation period is characterized by lower E_{pot} (3.49 mm /day, during the calibration period), higher precipitation (2.18 mm/day, versus 1.89), a higher precipitation frequency (λ=0.14 day^{-1}, versus 0.11) and a lower mean intensity (α=15.62 mm/event, versus 17.74). As the validation period precedes

the calibration period, this indicates a shift towards drier conditions. It is not known whether this change is reflected in vegetation properties, which would further help explain the difference in model performance. In any case, this illustrates the problems with transferring calibrated parameters to new conditions (Bartholomeus et al., 2015). Another particularity of this site is a high spatial heterogeneity of soil depth (Chiti et al., 2010), which is an additional challenge for predicting soil water balance at the scale of the entire site. Furthermore, Hickler et al. (2006) hypothesized that the vegetation has access to groundwater resources at this site, which would lead to an overestimation of the "reservoir" size in the calibration process. However, physiological indicators of water limitation observed at this site (Scartazza et al., 2013) suggest that the vegetation is at least partially dependent on the water stored in the unsaturated zone.

4.2 Behavior of the optimal rooting depth models

As can be seen on Figure 4, the optimality-based S_r agree quite well with the calibrated values at a majority of the sites. The cases where the difference is high will be discussed in the remaining paragraphs of this section. As in the illustrative examples of (Guswa, 2010), the results of both model versions are similar in most cases. The differences are highest at Lavarone, Renon and Lägeren. As seen on Figure 3, these sites are characterized by a similar precipitation regime (high mean intensity and intermediate frequency), and by the fact that P is greater than E_{pot} during the growing season. At Lavarone and Lägeren, the S_r values obtained with the conservative water use assumption (G10) are much closer to the calibrated values, while at Renon, the G10 estimate is much further from the calibrated values. However, as discussed later, this might indicate a general problem regarding the applicability of those models at this site (see below). Therefore, the limited evidence available here suggests that G10 version gives more plausible estimates of Z_e for energy-limited forests.

Among the sites with the greatest difference between modeled and calibrated S_r are the Mediterranean sites Roccarespampani and San Rossore (ellipse 1 on Fig. 7). As noted before, the performance of the water balance model was relatively low at these sites, which also reduces confidence in the calibrated S_r. Another possible explanation for the mismatch at Roccarespampani is that this site is a coppice, and thus its trees are very young (11 years at the beginning of measurements (Papale et al., 2015)). Therefore, the forest may be far from a steady state, making optimality-based model predictions less reliable. Also, coppiced systems tend to have a high root:total biomass fraction (Deckmyn et al., 2004), which might further explain the mismatch between modeled and calibrated S_r. At San Rossore, the presence of a water table at 1 to 2 m below ground (Papale et al., 2015) is another factor that may influence the rooting strategy of the vegetation. Indeed, the case where a plant sends deep roots in search of a water table is not covered by G08/G10 (Guswa, 2008). Glenz (2005) proposed a modeling strategy for those cases. Also, three of the sites where modeled and calibrated S_r differ most (San Rossore, Loobos and Le Bray – ellipse 2 on Fig. 7) are pine stands growing on sandy soils. *Pinus* roots often show a high degree of adaptation to soil conditions (Hacke et al., 2000; Kutschera and Lichtenegger, 2002). It is then conceivable that the carbon cost of roots decreases in coarser soils, allowing the trees to develop deeper roots than on finer soils. For example, doubling the L_r/D_r ratio to reflect cheaper roots (not shown) causes the value at Le Bray, Sodankylä and Hyytiälä

to be closer to the calibrated value. However, both L_r and D_r are difficult to observe and measurements are scarce, which makes it difficult to assess the plausibility of these parameter values. It is thus not possible to conclude how well G08 and G10 capture the rooting behavior of pines on sandy soils. It is also possible that the reason for deeper rooting systems in sandy soils is the avoidance of cavitation (Hacke et al., 2000), which is a different objective than the carbon budget optimization assumed here.

G08 and G10 estimate rooting depth based on water use optimization only, explicitly neglecting other constraints. According to Kutschera and Lichtenegger (2002), two of the main limitations to rooting depth are oxygen deficiency and low soil temperature. The latter applies primarily in temperate and cold climates, and may be amplified by high soil moisture content. In the temperature-dependent formulation proposed by Yang et al. (2016) and adopted here, low temperatures even promote root growth by decreasing the respiration costs. Norway spruce (*Picea abies*) is particularly sensitive to these factors, often causing it to form shallow rooting systems (Kutschera and Lichtenegger, 2002). This offers an explanation why the optimality-based S_r's are higher than the calibrated values at two of the three spruce sites. Indeed, the difference increases with increasing elevation between Tharandt (390 m asl), Wetzstein (703 m asl) and Renon (1794 m asl) (ellipse 3 on Fig. 7), which supports the hypothesis that the discrepancy is linked to temperature.

As seen on Fig. 4 b), the generic parameterization of Donohue et al. (2012) gives relatively good estimates of S_r when compared to the calibrated values, except at the sites where FORHYTM was found not to be applicable for the reasons discussed above. Some moderate tuning based on species-specific properties (Fig. 4 d)) improved the agreement somewhat, but did not change the general pattern. The vegetation parameters of G08/G10 are subject to a high degree of uncertainty. For example, photosynthetic water-use efficiency w_{ph} usually describes instantaneous gas exchange and can vary greatly with environmental conditions (Larcher, 2001), which makes its integration over a whole growing season challenging. Also, root length density D_r is required at the advancing root front. As rooting profiles usually follow an exponential distribution, this value is very small and subject to high measurement uncertainty. As seen on Fig. 4 d), a moderate change in the value of those parameters can have a strong influence on predicted S_r. Considering these uncertainty sources, we suggest using the generic parameterization unless detailed species or site-specific information is available.

4.3 Theoretical considerations

The G08 and G10 models are based on the assumption that plants dimension their rooting system to optimize their carbon budget. This involves processes taking place at the scale of an individual plant. However, these models were applied here at the scale of a community, thus neglecting any form of interactions between individuals. Various types of belowground interactions between forest trees have been reported, ranging from competition to facilitation (González de Andrés et al., 2017), and these interactions may alter root morphology and distribution (Bolte and Villanueva, 2006). Likewise, the interactions between overstory and understory roots are represented here in a very simplistic way, neglecting any form of competition. A somewhat related scaling issue arises from the fact that the model neglects the spatial heterogeneity of above- and belowground vegetation and soil properties. Both may influence the spatial distribution of soil moisture (Coenders-

Gerrits et al., 2013), and it is unclear to what extent their variability influences the average rooting depth over a forest stand. Such scaling issues are common in environmental modeling (Blöschl and Sivapalan, 1995), and the good agreement between calibrated S_r and G10 results suggests that the model may be applied at the stand scale despite the simplifications discussed in this paragraph.

The only difference between G08 and G10 is the function relating mean transpiration to rooting depth. While G08 assumes no transpiration regulation until soil moisture is fully depleted, G10 assumes that transpiration is linearly reduced as soon as soil moisture is no longer at saturation. As noted by Guswa (2010), these are two extreme assumptions, whereas most vegetation types show an intermediate behavior. Indeed, the reduction of transpiration when soil moisture is below a certain threshold is well documented for forests (Granier et al., 1999) and implemented in many dynamic models (Bergström, 1992; Granier et al., 1999; Zappa and Gurtz, 2003). The results of this study suggest that G10 better captures the behavior of forests under energy-limited conditions, whereas the water uptake strategy has little influence on estimated rooting depth under water-limited conditions.

4.4 Implications for model development

The good performance of the water balance model at temperate and cold sites suggests that the concept of a bulk S_r, defined as the product of soil water holding capacity and effective rooting depth, is an appropriate simplification of reality under these conditions. By contrast, FORHYTM failed to reproduce local water balance properly under Mediterranean climates and on dune soils, suggesting that the use of a bulk S_r is inappropriate at these locations. Accordingly, the difference between optimality-based and calibrated S_r was high at these sites.

The good agreement with calibrated values, at most sites where the use of S_r is considered appropriate, suggests that the G08/G10 model is a useful tool to parameterize S_r in temperate forests. For example, it can be used to constrain model calibration, thus contributing to reduce parameter uncertainty. Indeed, the meteorological data needed to calculate the climate parameters of G08/G10 belong to the data requirements of most hydrological models, and distributed estimates of LAI are available thanks to remote sensing. Also, soil water holding capacity κ may be estimated from soil properties such as texture and organic matter content, and is also commonly contained in distributed databases of soil properties (Tóth et al., 2017). Furthermore, the numerical approximation presented here for G10 (Eqs. 8-12) facilitates the implementation of the model. To our knowledge, the Michaelis-Menten equation has not been previously applied to hydrological processes. Another potential use of the G08/G10 model is the parameterization of a dynamic S_r in hydrological and ecohydrological models. This could greatly increase the credibility of climate impact projections (Montanari et al., 2013; Savenije and Hrachowitz, 2017).

Hydrol. Earth Syst. Sci. Discuss., https://doi.org/10.5194/hess-2017-723
Manuscript under review for journal Hydrol. Earth Syst. Sci.
Discussion started: 19 December 2017

5 Conclusion

In this study, we assessed the potential of an analytical, optimality-based rooting depth model to parameterize rooting zone storage capacity S_r in temperate forests. As observations of rooting profiles are scarce and performed at a spatial scale much smaller than the typical discretization unit in models, it was not possible to compare the results of the rooting depth function with direct measurements. Instead, S_r estimates were obtained by calibrating a water balance model against observations of latent heat flux and soil moisture at 15 eddy covariance stations. The results show a good agreement between optimality-based and calibrated S_r estimates at most of the sites where the use of S_r is a sensible simplification. However, this study suffers from a relatively small sample size. This was due to the strict criteria applied to site selection, applied to ensure a high level of reliability of the calibrated S_r estimates. These are still subject to some uncertainty, due to measurement uncertainty of the eddy covariance data, as well as parameter equifinality (Beven, 1993; Chaney et al., 2016). However, these two effects are inevitable to some extent, and the good performance of the water balance model suggests that this method provides appropriate ground-truth values at most sites. Where this is not the case, i.e. under Mediterranean climates and on very loose soils, the concept of S_r itself is probably inappropriate.

Despite the encouraging results obtained in this study, the results also show some potential for improvement of the optimal rooting depth model tested here. For example, specifying a penalty or limitation in cases of low soil temperature or oxygen stress would increase its applicability to cold regions and with species sensitive to these factors, such as *Picea abies*.

Data availability

This work used eddy covariance data acquired and shared by the FLUXNET community, including these networks: AmeriFlux, AfriFlux, AsiaFlux, CarboAfrica, CarboEuropeIP, CarboItaly, CarboMont, ChinaFlux, Fluxnet-Canada, GreenGrass, ICOS, KoFlux, LBA, NECC, OzFlux-TERN, TCOS-Siberia, and USCCC. The ERA-Interim reanalysis data are provided by ECMWF and processed by LSCE. The FLUXNET eddy covariance data processing and harmonization was carried out by the European Fluxes Database Cluster, AmeriFlux Management Project, and Fluxdata project of FLUXNET, with the support of CDIAC and ICOS Ecosystem Thematic Center, and the OzFlux, ChinaFlux and AsiaFlux offices.

An R code file containing an implementation of the methods described in this article is provided as a supplement.

Acknowledgments

This research was funded by the Swiss National Science Foundation (no. 153544) and the Swiss Federal Office for the Environment (no. 15.0003.PJ / Q104-0149). The authors would like to thank James Kirchner (ETH Zurich) for helpful comments on a previous version of this manuscript.

References

Anthoni, P.M., Knohl, A., Rebmann, C., Freibauer, A., Mund, M., Ziegler, W., Kolle, O., Schulze, E.-D., 2004. Forest and agricultural land-use-dependent CO2 exchange in Thuringia, Germany. Global Change Biology 10, 2005–2019. https://doi.org/10.1111/j.1365-2486.2004.00863.x

Aubinet, M., Chermanne, B., Vandenhaute, M., Longdoz, B., Yernaux, M., Laitat, E., 2001. Long term carbon dioxide exchange above a mixed forest in the Belgian Ardennes. Agricultural and Forest Meteorology 108, 293–315. https://doi.org/10.1016/S0168-1923(01)00244-1

Bai, Y., Zhang, J., Zhang, S., Koju, U.A., Yao, F., Igbawua, T., 2017. Using precipitation, vertical root distribution, and satellite-retrieved vegetation information to parameterize water stress in a Penman-Monteith approach to evapotranspiration modeling under Mediterranean climate. Journal of Advances in Modeling Earth Systems 9, 168–192. https://doi.org/10.1002/2016MS000702

Baldocchi, D., Falge, E., Gu, L., Olson, R., Hollinger, D., Running, S., Anthoni, P., Bernhofer, C., Davis, K., Evans, R., Fuentes, J., Goldstein, A., Katul, G., Law, B., Lee, X., Malhi, Y., Meyers, T., Munger, W., Oechel, W., Paw, K.T., Pilegaard, K., Schmid, H.P., Valentini, R., Verma, S., Vesala, T., Wilson, K., Wofsy, S., 2001. FLUXNET: A New Tool to Study the Temporal and Spatial Variability of Ecosystem–Scale Carbon Dioxide, Water Vapor, and Energy Flux Densities. Bulletin of the American Meteorological Society 82, 2415–2434. https://doi.org/10.1175/1520-0477(2001)082<2415:FANTTS>2.3.CO;2

Bartholomeus, R.P., Stagge, J.H., Tallaksen, L.M., Witte, J.P.M., 2015. Sensitivity of potential evaporation estimates to 100 years of climate variability. Hydrology and Earth System Sciences 19, 997–1014. https://doi.org/10.5194/hess-19-997-2015

Beachkofski, B., Grandhi, R., 2002. Improved Distributed Hypercube Sampling. American Institute of Aeronautics and Astronautics. https://doi.org/10.2514/6.2002-1274

Bergström, S., 1992. The HBV model - its structure and applications, SMHI Reports Hydrology. SMHI, Norrköping, Sweden.

Beven, K., 1993. Prophecy, reality and uncertainty in distributed hydrological modelling. Advances in Water Resources 16, 41–51. https://doi.org/10.1016/0309-1708(93)90028-E

Blöschl, G., Sivapalan, M., 1995. Scale issues in hydrological modelling: A review. Hydrological Processes 9, 251–290. https://doi.org/10.1002/hyp.3360090305

Bolte, A., Villanueva, I., 2006. Interspecific competition impacts on the morphology and distribution of fine roots in European beech (Fagus sylvatica L.) and Norway spruce (Picea abies (L.) Karst.). European Journal of Forest Research 125, 15–26. https://doi.org/10.1007/s10342-005-0075-5

Cescatti, A., Marcolla, B., 2004. Drag coefficient and turbulence intensity in conifer canopies. Agricultural and Forest Meteorology 121, 197–206. https://doi.org/10.1016/j.agrformet.2003.08.028

Chaney, N.W., Herman, J.D., Ek, M.B., Wood, E.F., 2016. Deriving global parameter estimates for the Noah land surface model using FLUXNET and machine learning: Improving Noah LSM Parameters. Journal of Geophysical Research: Atmospheres 121, 13,218–13,235. https://doi.org/10.1002/2016JD024821

Chaves, M.M., 2002. How Plants Cope with Water Stress in the Field? Photosynthesis and Growth. Annals of Botany 89, 907–916. https://doi.org/10.1093/aob/mcf105

Chiti, T., Papale, D., Smith, P., Dalmonech, D., Matteucci, G., Yeluripati, J., Rodeghiero, M., Valentini, R., 2010. Predicting changes in soil organic carbon in mediterranean and alpine forests during the Kyoto Protocol commitment periods using the CENTURY model: Changes in SOC in mediterranean and alpine forests. Soil Use and Management 26, 475–484. https://doi.org/10.1111/j.1475-2743.2010.00300.x

Coenders-Gerrits, A.M.J., Hopp, L., Savenije, H.H.G., Pfister, L., 2013. The effect of spatial throughfall patterns on soil moisture patterns at the hillslope scale. Hydrology and Earth System Sciences 17, 1749–1763. https://doi.org/10.5194/hess-17-1749-2013

de Boer-Euser, T., McMillan, H.K., Hrachowitz, M., Winsemius, H.C., Savenije, H.H.G., 2016. Influence of soil and climate on root zone storage capacity: ROOT ZONE STORAGE CAPACITY. Water Resources Research 52, 2009–2024. https://doi.org/10.1002/2015WR018115

Deckmyn, G., Laureysens, I., Garcia, J., Muys, B., Ceulemans, R., 2004. Poplar growth and yield in short rotation coppice: model simulations using the process model SECRETS. Biomass and Bioenergy 26, 221–227. https://doi.org/10.1016/S0961-9534(03)00121-1

Donohue, R.J., Roderick, M.L., McVicar, T.R., 2012. Roots, storms and soil pores: Incorporating key ecohydrological processes into Budyko's hydrological model. Journal of Hydrology 436-437, 35–50. https://doi.org/10.1016/j.jhydrol.2012.02.033

Eagleson, P.S., 1982. Ecological optimality in water-limited natural soil-vegetation systems: 1. Theory and hypothesis. Water Resources Research 18, 325–340. https://doi.org/10.1029/WR018i002p00325

Etzold, S., Ruehr, N.K., Zweifel, R., Dobbertin, M., Zingg, A., Pluess, P., Häsler, R., Eugster, W., Buchmann, N., 2011. The Carbon Balance of Two Contrasting Mountain Forest Ecosystems in Switzerland: Similar Annual Trends, but Seasonal Differences. Ecosystems 14, 1289–1309. https://doi.org/10.1007/s10021-011-9481-3

Federer, C.A., Vörösmarty, C., Fekete, B., 2003. Sensitivity of Annual Evaporation to Soil and Root Properties in Two Models of Contrasting Complexity. Journal of Hydrometeorology 4, 1276–1290. https://doi.org/10.1175/1525-7541(2003)004<1276:SOAETS>2.0.CO;2

Gao, H., Hrachowitz, M., Schymanski, S.J., Fenicia, F., Sriwongsitanon, N., Savenije, H.H.G., 2014. Climate controls how ecosystems size the root zone storage capacity at catchment scale: Root zone storage capacity in catchments. Geophysical Research Letters 41, 7916–7923. https://doi.org/10.1002/2014GL061668

Gentine, P., D'Odorico, P., Lintner, B.R., Sivandran, G., Salvucci, G., 2012. Interdependence of climate, soil, and vegetation as constrained by the Budyko curve. Geophysical Research Letters 39, n/a–n/a. https://doi.org/10.1029/2012GL053492

Glenz, C., 2005. Process-based, Spatially-explicit Modelling of Riparian Forest Dynamics in Central Europe – Tool for Decision-making in River Restoration. EPFL, Lausanne.

González de Andrés, E., Seely, B., Blanco, J.A., Imbert, J.B., Lo, Y.-H., Castillo, F.J., 2017. Increased complementarity in water-limited environments in Scots pine and European beech mixtures under climate change: Climate change increases complementarity in pine/beech mixedwoods. Ecohydrology 10, e1810. https://doi.org/10.1002/eco.1810

Granier, A., Bréda, N., Biron, P., Villette, S., 1999. A lumped water balance model to evaluate duration and intensity of drought constraints in forest stands. Ecological Modelling 116, 269–283. https://doi.org/10.1016/S0304-3800(98)00205-1

Granier, A., Reichstein, M., Bréda, N., Janssens, I.A., Falge, E., Ciais, P., Grünwald, T., Aubinet, M., Berbigier, P., Bernhofer, C., Buchmann, N., Facini, O., Grassi, G., Heinesch, B., Ilvesniemi, H., Keronen, P., Knohl, A., Köstner, B., Lagergren, F., Lindroth, A., Longdoz, B., Loustau, D., Mateus, J., Montagnani, L., Nys, C., Moors, E., Papale, D., Peiffer, M., Pilegaard, K., Pita, G., Pumpanen, J., Rambal, S., Rebmann, C., Rodrigues, A., Seufert, G., Tenhunen, J., Vesala, T., Wang, Q., 2007. Evidence for soil water control on carbon and water dynamics in European forests during the extremely dry year: 2003. Agricultural and Forest Meteorology 143, 123–145. https://doi.org/10.1016/j.agrformet.2006.12.004

Grünwald, T., Bernhofer, C., 2007. A decade of carbon, water and energy flux measurements of an old spruce forest at the Anchor Station Tharandt. Tellus B: Chemical and Physical Meteorology 59, 387–396. https://doi.org/10.1111/j.1600-0889.2007.00259.x

Guan, H., Wilson, J.L., 2009. A hybrid dual-source model for potential evaporation and transpiration partitioning. Journal of Hydrology 377, 405–416. https://doi.org/10.1016/j.jhydrol.2009.08.037

Gupta, H.V., Kling, H., Yilmaz, K.K., Martinez, G.F., 2009. Decomposition of the mean squared error and NSE performance criteria: Implications for improving hydrological modelling. Journal of Hydrology 377, 80–91. https://doi.org/10.1016/j.jhydrol.2009.08.003

Guswa, A.J., 2010. Effect of plant uptake strategy on the water-optimal root depth. Water Resources Research 46. https://doi.org/10.1029/2010WR009122

Guswa, A.J., 2008. The influence of climate on root depth: A carbon cost-benefit analysis. Water Resources Research 44, n/a–n/a. https://doi.org/10.1029/2007WR006384

Hacke, U.G., Sperry, J.S., Ewers, B.E., Ellsworth, D.S., Schäfer, K.V.R., Oren, R., 2000. Influence of soil porosity on water use in Pinus taeda. Oecologia 124, 495–505. https://doi.org/10.1007/PL00008875

Hickler, T., Prentice, I.C., Smith, B., Sykes, M.T., Zaehle, S., 2006. Implementing plant hydraulic architecture within the LPJ Dynamic Global Vegetation Model. Global Ecology and Biogeography 15, 567–577. https://doi.org/10.1111/j.1466-

8238.2006.00254.x

Jarvis, P.G., 1976. The interpretation of the variations in leaf water potential and stomatal conductance found in canopies in the field. Phil. Trans. Royal Soc. London B 273, 593–610.

Kalliokoski, T., Pennanen, T., Nygren, P., Sievänen, R., Helmisaari, H.-S., 2010. Belowground interspecific competition in mixed boreal forests: fine root and ectomycorrhiza characteristics along stand developmental stage and soil fertility gradients. Plant and Soil 330, 73–89. https://doi.org/10.1007/s11104-009-0177-9

Keller, T., 1967. Beitrag zur Kenntnis der Wurzelatmung von Koniferenjungpflanzen, in: Proc. from XIV IUFRO-Congress. Munich, pp. 329–340.

Kleidon, A., Heimann, M., 1998. A method of determining rooting depth from a terrestrial biosphere model and its impacts on the global water and carbon cycle. Global Change Biology 4, 275–286. https://doi.org/10.1046/j.1365-2486.1998.00152.x

Kling, H., Fuchs, M., Paulin, M., 2012. Runoff conditions in the upper Danube basin under an ensemble of climate change scenarios. Journal of Hydrology 424-425, 264–277. https://doi.org/10.1016/j.jhydrol.2012.01.011

Köppen, W., 2011. The thermal zones of the Earth according to the duration of hot, moderate and cold periods and to the impact of heat on the organic world. Meteorologische Zeitschrift 20, 351–360. https://doi.org/10.1127/0941-2948/2011/105

Kramer, K., 1996. Phenology and growth of European trees in relation to climate change. Landbouw Universiteit, Wageningen, The Netherlands.

Kramer, K., Leinonen, I., Bartelink, H.H., Berbigier, P., Borghetti, M., Bernhofer, C., Cienciala, E., Dolman, A.J., Froer, O., Gracia, C.A., Granier, A., Grunwald, T., Hari, P., Jans, W., Kellomaki, S., Loustau, D., Magnani, F., Markkanen, T., Matteucci, G., Mohren, G.M.J., Moors, E., Nissinen, A., Peltola, H., Sabate, S., Sanchez, A., Sontag, M., Valentini, R., Vesala, T., 2002. Evaluation of six process-based forest growth models using eddy-covariance measurements of CO2 and H2O fluxes at six forest sites in Europe. Global Change Biology 8, 213–230. https://doi.org/10.1046/j.1365-2486.2002.00471.x

Kutschera, L., Lichtenegger, E., 2002. Wurzelatlas mitteleuropäischer Waldbäume und Sträucher, 2. Aufl. ed, Wurzelatlas-Reihe. Stocker, Graz.

Larcher, W., 2001. Ökophysiologie der Pflanzen: Leben, Leistung und Streßbewältigung der Pflanzen in ihrer Umwelt ; 77 Tabellen, 8 Boxen, 6., neubearb. Aufl. ed, UTB für Wissenschaft. Ulmer, Stuttgart.

Lindroth, A., Lagergren, F., Aurela, M., Bjarnadottir, B., Christensen, T., Dellwik, E., Grelle, A., Ibrom, A., Johansson, T., Lankreijer, H., Launiainen, S., Laurila, T., MöLder, M., Nikinmaa, E., Pilegaard, K., Sigurdsson, B.D., Vesala, T., 2008. Leaf area index is the principal scaling parameter for both gross photosynthesis and ecosystem respiration of Northern deciduous and coniferous forests. Tellus B 60, 129–142. https://doi.org/10.1111/j.1600-0889.2007.00330.x

Loustau, D., Bosc, A., Colin, A., Ogee, J., Davi, H., Francois, C., Dufrene, E., Deque, M., Cloppet, E., Arrouays, D., Le Bas, C., Saby, N., Pignard, G., Hamza, N., Granier, A., Breda, N., Ciais, P., Viovy, N., Delage, F., 2005. Modeling climate change effects on the potential production of French plains forests at the sub-regional level. Tree Physiology 25, 813–823. https://doi.org/10.1093/treephys/25.7.813

Menzel, L., 1997. Modellierung der Evapotranspiration im System Boden-Pflanze-Atmosphäre, Zürcher Geographische Schriften. ETH Zurich.

Miller, G.R., Baldocchi, D.D., Law, B.E., Meyers, T., 2007. An analysis of soil moisture dynamics using multi-year data from a network of micrometeorological observation sites. Advances in Water Resources 30, 1065–1081. https://doi.org/10.1016/j.advwatres.2006.10.002

Milly, P.C.D., 1994. Climate, soil water storage, and the average annual water balance. Water Resources Research 30, 2143–2156. https://doi.org/10.1029/94WR00586

Milly, P.C.D., 1993. An analytic solution of the stochastic storage problem applicable to soil water. Water Resources Research 29, 3755–3758. https://doi.org/10.1029/93WR01934

Montanari, A., Young, G., Savenije, H.H.G., Hughes, D., Wagener, T., Ren, L.L., Koutsoyiannis, D., Cudennec, C., Toth, E., Grimaldi, S., Blöschl, G., Sivapalan, M., Beven, K., Gupta, H., Hipsey, M., Schaefli, B., Arheimer, B., Boegh, E., Schymanski, S.J., Di Baldassarre, G., Yu, B., Hubert, P., Huang, Y., Schumann, A., Post, D.A., Srinivasan, V., Harman, C., Thompson, S., Rogger, M., Viglione, A., McMillan, H., Characklis, G., Pang, Z., Belyaev, V., 2013. "Panta Rhei—Everything Flows": Change in hydrology and society—The IAHS Scientific Decade 2013–2022. Hydrological Sciences Journal 58, 1256–1275. https://doi.org/10.1080/02626667.2013.809088

Morillas, L., Leuning, R., Villagarcía, L., García, M., Serrano-Ortiz, P., Domingo, F., 2013. Improving evapotranspiration estimates in Mediterranean drylands: The role of soil evaporation: Evapotranspiration Estimation in Mediterranean Dry Lands. Water Resources Research 49, 6572–6586. https://doi.org/10.1002/wrcr.20468

Nijzink, R., Hutton, C., Pechlivanidis, I., Capell, R., Arheimer, B., Freer, J., Han, D., Wagener, T., McGuire, K., Savenije, H., Hrachowitz, M., 2016. The evolution of root-zone moisture capacities after deforestation: a step towards hydrological predictions under change? Hydrology and Earth System Sciences 20, 4775–4799. https://doi.org/10.5194/hess-20-4775-2016

Papale, D., Migliavacca, M., Cremonese, E., Cescatti, A., Alberti, G., Balzarolo, M., Belelli Marchesini, L., Canfora, E., Casa, R., Duce, P., Facini, O., Galvagno, M., Genesio, L., Gianelle, D., Magliulo, V., Matteucci, G., Montagnani, L., Petrella, F., Pitacco, A., Seufert, G., Spano, D., Stefani, P., Vaccari, F.P., Valentini, R., 2015. Carbon, Water and Energy Fluxes of Terrestrial Ecosystems in Italy, in: Valentini, R., Miglietta, F. (Eds.), The Greenhouse Gas Balance of Italy. Springer Berlin Heidelberg, Berlin, Heidelberg, pp. 11–45.

Penman, H.L., 1948. Natural evaporation from open water, bare soil and grass. Proceedings of the Royal Society 193, 120–146.

Polster, H., 1950. Die physiologischen Grundlagen der Stofferzeugung im Walde. Untersuchungen über Assimilation, Respiration und Transpiration unserer Hauptholzarten. Bayerischer Landwirtschaftsverlag GmbH, Munich.

Porporato, Daly, Rodriguez-Iturbe, 2004. Soil Water Balance and Ecosystem Response to Climate Change. The American Naturalist 164, 625. https://doi.org/10.2307/3473173

Rodriguez-Iturbe, I., Porporato, A., Ridolfi, L., Isham, V., Coxi, D.R., 1999. Probabilistic modelling of water balance at a point: the role of climate, soil and vegetation. Proceedings of the Royal Society A: Mathematical, Physical and Engineering

Sciences 455, 3789–3805. https://doi.org/10.1098/rspa.1999.0477

Savenije, H.H.G., Hrachowitz, M., 2017. HESS Opinions "Catchments as meta-organisms - a new blueprint for hydrological modelling." Hydrology and Earth System Sciences 21, 1107–1116. https://doi.org/10.5194/hess-21-1107-2017

Scartazza, A., Moscatello, S., Matteucci, G., Battistelli, A., Brugnoli, E., 2013. Seasonal and inter-annual dynamics of growth, non-structural carbohydrates and C stable isotopes in a Mediterranean beech forest. Tree Physiology 33, 730–742. https://doi.org/10.1093/treephys/tpt045

Schymanski, S.J., Sivapalan, M., Roderick, M.L., Hutley, L.B., Beringer, J., 2009. An optimality-based model of the dynamic feedbacks between natural vegetation and the water balance. Water Resources Research 45, n/a–n/a. https://doi.org/10.1029/2008WR006841

Smettem, K., Callow, N., 2014. Impact of Forest Cover and Aridity on the Interplay between Effective Rooting Depth and Annual Runoff in South-West Western Australia. Water 6, 2539–2551. https://doi.org/10.3390/w6092539

Speich, M.J.R., Zappa, M., Lischke, H., n.d. Sensitivity of forest water balance and physiological drought predictions to soil and vegetation parameters – a model-based study. Under review for Environmental Modelling and Software.

Sprenger, M., Volkmann, T.H.M., Blume, T., Weiler, M., 2015. Estimating flow and transport parameters in the unsaturated zone with pore water stable isotopes. Hydrology and Earth System Sciences 19, 2617–2635. https://doi.org/10.5194/hess-19-2617-2015

Stewart, J.., 1988. Modelling surface conductance of pine forest. Agricultural and Forest Meteorology 43, 19–35. https://doi.org/10.1016/0168-1923(88)90003-2

Tóth, B., Weynants, M., Pásztor, L., Hengl, T., 2017. 3D soil hydraulic database of Europe at 250 m resolution. Hydrological Processes 31, 2662–2666. https://doi.org/10.1002/hyp.11203

Valentini, R., Angelis, P., Matteucci, G., Monaco, R., Dore, S., Mucnozza, G.E.S., 1996. Seasonal net carbon dioxide exchange of a beech forest with the atmosphere. Global Change Biology 2, 199–207. https://doi.org/10.1111/j.1365-2486.1996.tb00072.x

Valladares, F., Niinemets, Ü., 2008. Shade Tolerance, a Key Plant Feature of Complex Nature and Consequences. Annual Review of Ecology, Evolution, and Systematics 39, 237–257. https://doi.org/10.1146/annurev.ecolsys.39.110707.173506

Vegas–Galdos, F., Alvarez, C., Garcia, A., Revilla, J.A., 2012. Estimated distributed rainfall interception using a simple conceptual model and Moderate Resolution Imaging Spectroradiometer (MODIS). Journal of Hydrology 468–498, 213–228.

Wang-Erlandsson, L., Bastiaanssen, W.G.M., Gao, H., Jägermeyr, J., Senay, G.B., van Dijk, A.I.J.M., Guerschman, J.P., Keys, P.W., Gordon, L.J., Savenije, H.H.G., 2016. Global root zone storage capacity from satellite-based evaporation. Hydrology and Earth System Sciences 20, 1459–1481. https://doi.org/10.5194/hess-20-1459-2016

Wang, K., Dickinson, R.E., 2012. A review of global terrestrial evapotranspiration: Observation, modeling, climatology, and climatic variability. Reviews of Geophysics 50. https://doi.org/10.1029/2011RG000373

Wang, Q., Tenhunen, J., Dinh, N., Reichstein, M., Otieno, D., Granier, A., Pilegarrd, K., 2005. Evaluation of seasonal variation of MODIS derived leaf area index at two European deciduous broadleaf forest sites. Remote Sensing of

Environment 96, 475–484. https://doi.org/10.1016/j.rse.2005.04.003

Weisstein, E.W., n.d. Incomplete Gamma Function [WWW Document]. URL http://mathworld.wolfram.com/IncompleteGammaFunction.html (accessed 6.22.17).

Withington, J.M., Reich, P.B., Oleksyn, J., Eissenstat, D.M., 2006. Comparisons of structure and life span in roots and leaves among temperate trees. Ecological Monographs 76, 381–397. https://doi.org/10.1890/0012-9615(2006)076[0381:COSALS]2.0.CO;2

Yang, Y., Donohue, R.J., McVicar, T.R., 2016. Global estimation of effective plant rooting depth: Implications for hydrological modelling. Water Resources Research. https://doi.org/10.1002/2016WR019392

Zappa, M., Gurtz, J., 2003. Simulation of soil moisture and evapotranspiration in a soil profile during the 1999 MAP-Riviera Campaign. Hydrology and Earth System Sciences 7, 903–919. https://doi.org/10.5194/hess-7-903-2003

Zierl, B., 2001. A water balance model to simulate drought in forested ecosystems and its application to the entire forested area in Switzerland. Journal of Hydrology 242, 115–136. https://doi.org/10.1016/S0022-1694(00)00387-5